4. Results

4.1. Biopsy material

Biopsy specimen before treatment showed that the tumor exhibited features of mucinous (colloid) carcinoma, being comprised of islands and strips of columnar cells floating in large pools of extracellular mucin (Fig. 2). The extracellular mucin was stained by Alcian-blue staining with hyaluronidase resistance (data not shown).

4.2. Autopsy material

A tumor exceeding 10 cm in diameter was identified in the anterior mediastinum. Macroscopically, the tumor was uncapsulated and white. The tumor had clear margins and was clearly isolated from the lung. Partial resection of the tumor was performed.

In the autopsy specimens, the tumor showed acinar and cribriform structure [Fig. 3(A)]. The tumor was composed of tall columnar cells, with varying amounts of cytoplasmic mucin [Fig. 3(B)]. No keratinization was observed. No normal thymic tissue or accompanying thymoma was found in the specimens.

The immunohistochemical findings are shown in Table 1. Most tumor cells were positive for cytokeratin (CK) 7 [Fig. 3(C)] but negative for CK20. The tumor cells were partially positive for CD5 [Fig. 3(D)]. The extracellular mucin and tumor cells were strongly positive for MUC5AC and were partially positive for MUC6. They were negative for markers for pulmonary, mesothelial, germ cell, neuroendocrine, squamous cell, and/or large intestine differentiation. Stromal infiltrating lymphocytes were negative for TdT, CD1a, and/or CD99.

5. Discussion

Primary carcinomas of the thymus are uncommon, and when diagnosed, majority are squamous cell carcinomas or its variants [1]. Although histochemical and immunohistochemical evidence for glandular differentiation is described in thymic carcinoma [5], primary adenocarcinomas of the thymus remain very rare, with only 9 cases have been reported to date [2-4]. Only one case of mucinous adenocarcinoma of the thymus has been reported previously [4].

Because primary thymic adenocarcinoma is so rare, it is necessary to consider other diagnostic possibilities, such as variants of other thymic tumors, metastatic adenocarcinoma, mesothelioma, and germ cell tumors. Other kinds of primary thymic tumors with abundant mucin, such as carcinoid with prominent mucinous stroma and mucoepidermoid carcinoma, should also be considered as differential diagnosis [6]. The carcinoid with prominent mucinous stroma was composed of a conventional neuroendocrine morphology such as an organoid pattern and delicate fibrovascular septa, and immunoreactivity for pan-neuroendocrine markers. For a tumor to be diagnosed as mucoepidermoid carcinoma, both the squamous and the mucin-producing components should be cytologically bland. That was not the case in the presented tumor.

It is important to discriminate between primary and metastatic thymic adenocarcinoma. Metastatic adenocarcinoma of the thymus usually arises from the respiratory or upper alimentary tracts, although other sites of origin have also been reported [7].

Expression of TTF-1, SP-A, and napsin A are known to be specific markers for ordinary pulmonary adenocarcinoma [8,9]. However, this case was negative for these markers. Pulmonary mucin-rich neoplasms include mucinous–bronchioloalveolar carcinoma (m-BAC) and mucinous cyst adenocarcinoma. Mucinous–bronchioloalveolar carcinomas had been called goblet cell–type adenocarcinoma and are growing along alveolar walls and without stromal invasion [10]. It tends to spread aerogenously, forming satellite tumors. Immunohistochemically, m-BAC is known to express MUC5AC, but low immunoreactivity for TTF-1 was reported [11]. This case partially resembled m-BAC by exhibiting similar pattern of immunohistochemical findings including being MUC5AC-positive and TTF-1–negative. However, m-BAC frequently displays pneumonialike distribution in the clinical setting [10]. The tumor of this patient was localized in the anterior mediastinum and was clearly isolated from the lung parenchyma. Mucinous cyst adenocarcinoma of the lung is extremely rare tumor and showed coordinated overexpression of CDX2 and MUC2 but only partially retained the markers of pulmonary origin [12]. This case was negative for CDX-2, MUC2, TTF-1, SP-A, and napsin A. Based on these findings, the possibility of pulmonary origin of our patient's tumor was considered to be extremely low.

Other mucin-rich neoplasms include those of the gastrointestinal tract, ovary, pancreas, and breast. Mucinous carcinoma of the breast and pancreas is known to express MUC2. However, this case was negative for MUC2. In addition, clinical and radiographic examinations including endoscopic gastroenterologic findings disclosed no evidence of tumor elsewhere. Therefore, the possibility of metastasis from these organs was also considered to be extremely low.

MUC5AC is expressed by gastric foveolar cells and MUC6 by pyloric gland cells [13]. In the presented case, tumor cells and extracellular mucin were strongly positive for MUC5AC and partially positive for MUC6, suggesting that this tumor produces the gastric-type mucin. As for this particular case, gastric carcinoma was not clinically identified. Thus, it is worthy to note that our findings on the expression of MUC5AC and MUC6 by thymic tumor are of interest because there has been no studies reported on this matter to the best of our knowledge.

There are no immunohistological markers specific for tumors of thymic origin. The lymphocyte marker

CD5 is expressed in approximately 70% of all cases of thymic carcinoma and is uncommon in nonthymic carcinomas, although the frequency of expression of CD5 in extrathymic adenocarcinomas has been disputed [14].

Immunohistochemically, the presented case was revealed to be diffusely positive for CK7 and focally positive for CD5. These results resemble the case reported by Choi et al [4], which demonstrated focal positive staining for CD5 providing further support for thymic origin. In conclusion, the diagnosis of this case was primary mucinous adenocarcinoma of the thymus. This case demonstrated that the mucinous subtype should be considered as one of the histopathological entities of thymic adenocarcinoma. We postulate that this is a major consideration of importance.

Acknowledgments

We would like to thank Dr Ishii, Ms Shimizu, Dr Kunogi, Kubota, Yahata, Suzuki, and Dr Kodama for their excellent support.

References

[1] Suster S, Moran CA. Thymic carcinoma: spectrum of differentiation and histologic types. Pathology 1998;30:111-22.

[2] Babu MK, Nirmala V. Thymic carcinoma with glandular differentiation arising in a congenital thymic cyst. J Surg Oncol 1994; 57:277-9.

[3] Matsuno Y, Morozumi N, Hirohashi S, et al. Papillary carcinoma of the thymus: report of four cases of a new microscopic type of thymic carcinoma. Am J Surg Pathol 1998;22:873-80.

[4] Choi WW, Lui YH, Lau WH, et al. Adenocarcinoma of the thymus: report of two cases, including a previously undescribed mucinous subtype. Am J Surg Pathol 2003;27:124-30.

[5] Matsuno Y, Mukai K, Noguchi M, et al. Histochemical and immunohistochemical evidence of glandular differentiation in thymic carcinoma. Acta Pathol Jpn 1989;39:433-48.

[6] Suster S, Moran CA. Thymic carcinoid with prominent mucinous stroma. Report of a distinctive morphologic variant of thymic neuroendocrine neoplasm. Am J Surg Pathol 1995;19:1277-85.

[7] Ritter JH, Wick MR. Primary carcinomas of the thymus gland. Semin Diagn Pathol 1999;16:18-31.

[8] Chhieng DC, Cangiarella JF, Zakowski MF, et al. Use of thyroid transcription factor 1, PE-10, and cytokeratins 7 and 20 in discriminating between primary lung carcinomas and metastatic lesions in fine-needle aspiration biopsy specimens. Cancer 2001;93:330-6.

[9] Hirano T, Auer G, Maeda M, et al. Human tissue distribution of TA02, which is homologous with a new type of aspartic proteinase, napsin A. Jpn J Cancer Res 2000;91:1015-21.

[10] Gemma A, Noguchi M, Hirohashi S, et al. Clinicopathologic and immunohistochemical characteristics of goblet cell type adenocarcinoma of the lung. Acta Pathol Jpn 1991;41:737-43.

[11] Copin MC, Buisine MP, Leteurtre E, et al. Mucinous bronchioloalveolar carcinomas display a specific pattern of mucin gene expression among primary lung adenocarcinomas. Hum Pathol 2001;32:274-81.

[12] Rossi G, Murer B, Cavazza A, et al. Primary mucinous (so-called colloid) carcinomas of the lung: a clinicopathologic and immunohistochemical study with special reference to CDX-2 homeobox gene and MUC2 expression. Am J Surg Pathol 2004;28:442-52.

[13] De Bolos C, Garrido M, Real FX. MUC6 apomucin shows a distinct normal tissue distribution that correlates with Lewis antigen expression in the human stomach. Gastroenterology 1995;109:723-34.

[14] Kornstein MJ, Rosai J. CD5 labeling of thymic carcinomas and other nonlymphoid neoplasms. Am J Clin Pathol 1998;109:722-6.

VOLUME 24 · NUMBER 1 · JANUARY 1 2006

JOURNAL OF CLINICAL ONCOLOGY

ORIGINAL REPORT

Neuroendocrine Neoplasms of the Lung: A Prognostic Spectrum

Hisao Asamura, Toru Kameya, Yoshihiro Matsuno, Masayuki Noguchi, Hirohito Tada, Yuichi Ishikawa, Tomoyuki Yokose, Shi-Xu Jiang, Takeshi Inoue, Ken Nakagawa, Kinuko Tajima, and Kanji Nagai

From the National Cancer Center Hospital; The Cancer Institute Hospital, Tokyo; National Cancer Center East, Chiba; Shizuoka Cancer Center, Shizuoka; Kitasato University School of Medicine, Kitasato; Tsukuba University School of Medicine, Tsukuba; Sanritsu Co, Chiba; and Osaka City General Hospital, Osaka, Japan.

Submitted September 5, 2005; accepted October 5, 2005.

Supported in part by a Grant-in-Aid No. 11-19 for Cancer Research from the Ministry of Health and Welfare, Japan.

Authors' disclosures of potential conflicts of interest and author contributions are found at the end of this article.

Address reprint requests to Hisao Asamura, Division of Thoracic Surgery, National Cancer Center Hospital, 1-1, Tsukiji 5-chome, Chuo-ku, Tokyo 104-0045, Japan; e-mail: hasamura@ncc.go.jp.

0732-183X/06/2401-70/$20.00

DOI: 10.1200/JCO.2005.04.1202

ABSTRACT

Purpose
Neuroendocrine (NE) tumors of the lung include typical carcinoid (TC), atypical carcinoid (AC), large-cell NE carcinoma (LCNEC), and small-cell lung carcinoma (SCLC). Their clinicopathologic profiles and relative grade of malignancy have not been defined.

Patients and Methods
From 10 Japanese institutes, 383 surgically resected pulmonary NE tumors were collected. The histologic diagnosis was determined by the consensus of a pathology panel consisting of six expert pathologists as TC, AC, LCNEC, or SCLC on the basis of the WHO classification, and its relationship to clinicopathologic profiles was analyzed.

Results
Of the 383 tumors, 18 were excluded because of an improper specimen. The pathology panel reviewed the remaining 366 tumors, and a diagnosis of NE tumor was made in 318 patients (87.4%); 55 patients had TC, nine had AC, 141 had LCNEC, and 113 had SCLC. The 5-year survival rates of patients with all stages were as follows: 96.2% for TC, 77.8% for AC, 40.3% for LCNEC, and 35.7% for SCLC. There was significant prognostic difference between TC and AC as well as between AC and LCNEC+SCLC. However, there was no difference between LCNEC and SCLC, and their survival curves were superimposed. The multivariate analysis indicated that histologic type, completeness of resection, symptoms, nodal involvement, and age were significantly prognostic.

Conclusion
The grade of malignancy of NE tumors was upgraded in the following order: TC, AC, LCNEC, and SCLC. No prognostic difference was noted between LCNEC and SCLC. The high-grade NE histology uniformly indicated poor prognosis regardless of its histologic type.

J Clin Oncol 24:70-76. © 2006 by American Society of Clinical Oncology

INTRODUCTION

Normal lung contains a population of neuroendocrine cells, where the term neuroendocrine (NE) defines a specific group of cells based on their secretory products, distinct staining characteristics, and ability to uptake and decarboxylate amine precursors.[1] Lung tumors originating from NE cells or differentiating into NE cells have been recognized, and they are represented by a wide range of pathologic entities.[2-5] It is now widely recognized that NE tumors of the lung include a spectrum, from low-grade typical carcinoid (TC) to intermediate-grade atypical carcinoid (AC) to high-grade large-cell NE carcinoma (LCNEC) and small-cell lung carcinoma (SCLC).[2-5] LCNEC is a unique tumor that shows immunohistochemical and morphologic appearance as high-grade NE tumors and non–small-cell nuclear features. Its clinicopathologic behaviors have been elucidated only recently.[5-12]

In the recent revision of the WHO classification of lung and pleural tumors, the same grading was adopted with detailed criteria for each subtype of NE tumors, although LCNEC was subcategorized as a type of large-cell carcinoma.[13] However, the important issues regarding NE tumors of the lung have not yet been defined. In particular, the grade of malignancy of each NE subtype has not been defined. There is little information available on the relative grade of malignancy among the several histologic types. However, to ensure the appropriate choice of treatment strategy for patients with various types of NE lung tumors, a histology-specific understanding of clinicopathologic behavior and prognosis is indispensable.

Considering the importance of histologic diagnoses and their reproducibility, this study was conducted in a retrospective, multi-institutional setting with a critical review of histology by an expert panel. The clinicopathologic background

of patients was collected, and histology-specific characteristics were extensively analyzed.

PATIENTS AND METHODS

Patients

A total of 383 patients with a histologic diagnosis of primary pulmonary NE tumor at each institution were enrolled onto this retrospective study. Intermediate- and high-grade NE tumors were a focus for enrollment. Samples were obtained from 10 institutions in the Japanese Multicenter Study Group of NE Tumors (Appendix). To ensure that there would be enough specimens for pathologic examination, only surgical cases were considered. Patients who were diagnosed only by biopsy sample and treated by some modality other than surgery were excluded. Histopathologic and clinicopathologic studies were performed. The final histologic diagnosis was established by an expert central review, as described later in detail. Extensive clinical information was also collected and included demographic data, surgical information, preoperative serum tumor marker levels, pathologic data, endocrine syndromes (Cushing's syndrome, acromegaly, and so on), tumor recurrence, and survival. For serum tumor markers, three markers, carcinoembryonic antigen (CEA; normal range, < 5 ng/mL), neuron-specific enolase (NSE; normal range, < 15 ng/mL), and progastrin-releasing peptide (proGRP; normal range, < 46 ng/mL), were studied. All patients were staged postsurgically according to the International Union Against Cancer TNM classification system.[13]

Pathologic Diagnosis: Central Review

To ensure an accurate histologic diagnosis as NE tumor, the histology of all of the enrolled patients was reviewed by a pathology panel consisting of six experts (T.K., Y.M., T.I., Y.I., M.N., and T.Y.). Paraffin-embedded blocks or unstained slide glasses were obtained in all cases and processed by routine hematoxylin and eosin staining and immunohistochemical studies solely at one institution (T.K. and S.-X.J.). To demonstrate the NE phenotype, at least three antibodies to chromogranin-A, CD56 (neural adhesion molecule), and synaptophysin were used. Immunohistochemically, the tumor was considered as positive if the tumor cells exhibited focal, patchy, or diffuse staining in the intracellular locations for each antigen. The classification criteria were based on the revised WHO classification of lung carcinoma (1999),[14] in which TC, AC, LCNEC, and SCLC are strictly differentiated. The process of central review was as follows. First, the pathology panel members performed a pathology review independently, and their respective reports were sent directly to the central office. After the individual reviews were completed, a review meeting was held to establish a final consensus on the histologic type in each case. The evaluation of immunohistochemical staining was also documented.

Statistics

The Kaplan-Meier product limit estimator was used to graphically display the survival curves, and the log-rank test was used to compare survival between different groups. The Cox proportional hazard model was used to examine the effects of variables that may have affected the prognosis of patients with NE tumors. $P \leq .05$ was considered significant.

RESULTS

Among the 383 patients enrolled, 18 were excluded from the study. In 17 patients, the specimens were judged to be inappropriate because either the tumors were of nonpulmonary origin or no specimens were available from the primary site. In one patient, the eligibility criteria were not met because this was an autopsy case. The remaining 365 tumors were considered for further central pathology review.

Central Pathology Review

Of the 365 tumors, as a final agreement of the review meetings, a total of 318 (87.1%) were diagnosed as pulmonary NE tumors, whereas a histology of non-NE tumor was confirmed in 47 tumors (12.9%; Table 1). Actually, the pathology panel could not reach a consensus with regard to the histologic type of 14 high-grade NE tumors at the initial session of panel meetings. Therefore, after enough intervals, the panel meetings were held again, and the final consensus as either LCNEC or SCLC was established. Of the NE tumors, a diagnosis of TC, AC, LCNEC, and SCLC was made in 55, nine, 141, and 113 patients, respectively. In the non-NE tumors, large-cell carcinoma (LCC) was most commonly seen (33 patients), followed by poorly differentiated squamous cell carcinoma (seven patients), poorly differentiated adenocarcinoma (three patients), pulmonary blastoma (two patients), and indeterminate histology by treatment (two patients). When looking at the histologic subtypes of 74 LCCs, 141 were diagnosed as LCNEC because of the coexistence of NE morphology and phenotype. However, the NE phenotype was not demonstrated despite the presence of NE morphology in 11 patients (LCC with NE morphology), and the NE morphology was not demonstrated despite the presence of NE phenotype in 12 patients (LCC with NE phenotype). In the remaining 10 patients, neither NE phenotype nor NE morphology was demonstrated (LCC). Among 141 LCNECs, 15 tumors (10.6%) were combined with other histologic types, and 126 tumors (89.14%) were not combined (Table 2). Also, among 113 SCLCs, 30 tumors (26.6%) were combined with other histologic types, and 83 tumors (73.4%) were not combined (Table 3). Despite the various combinations of high-grade NE tumors with other histologic types, neither TC nor AC was seen as the combined histology for LCNEC and SCLC.

Clinicopathologic Profiles

The clinical background and profiles were studied according to the histologic type (Table 4). Aggressive tumors tended to affect older patients. In particular, patients with TC were significantly younger than patients with other tumor histologies. A remarkable difference in sex distribution was seen between carcinoid tumors (TC and AC) and other high-grade NE carcinomas (LCNEC and SCLC). Compared with carcinoid tumors, the high-grade NE tumors affected men significantly more often than women, with males accounting for more than 80% to 90% of the tumors. Also, 95% to 100% of the patients with high-grade NE carcinomas had a smoking history, whereas only half of the patients with carcinoid tumors were smokers. Only four patients (1.3%) in the entire group of patients with NE tumors showed

Table 1. Histologic Diagnosis

Histologic Type	No. of Patients	%
NE tumors	318	87.1
TC	55	15.1
AC	9	2.5
LCNEC	141	38.6
SCLC	113	31.0
Non-NE tumors	47	12.9
LCC	33	9.0
Others	14	3.8
Total	365	100

Abbreviations: NE, neuroendocrine; TC, typical carcinoid; AC, atypical carcinoid; LCNEC, large-cell neuroendocrine carcinoma; SCLC, small-cell lung carcinoma; LCC, large-cell carcinoma.

Table 2. Details of Histologic Diagnosis of LCNEC

Histologic Type	No. of Patients	%
LCNEC, not combined	126	89.4
LCNEC, combined	15	10.6
With AD	5	3.5
With SQ	8	5.7
With others	2	1.4
Total	141	100

Abbreviations: LCNEC, large-cell neuroendocrine carcinoma; SCLC, small-cell lung carcinoma; AD, adenocarcinoma; SQ, squamous-cell carcinoma.

symptoms related to the paraneoplastic syndromes. The following syndromes were seen: Eaton-Lambert's syndrome in two patients with SCLC, syndrome of inappropriate antidiuretic hormone secretion in one patient with SCLC, and carcinoid syndrome in one patient with TC. In AC and LCNEC, paraneoplastic syndrome was not seen. The serum tumor markers of CEA, NSE, and proGRP were measured before surgery in 298 (93.7%), 240 (75.5%), and 79 (24.8%) of 318 patients, respectively (Table 5). The serum CEA level was elevated in half of the patients with LCNEC or SCLC. Although proGRP was a good marker of high-grade NE tumors, the elevation of NSE level was limited in these patients, probably because of the relatively early stage for the tumors. The pathologic profiles of resected tumors are listed in Table 6. The average size of LCNEC (41 mm) was the largest among NE tumors; other types averaged approximately 30 mm in diameter. In TC, nodal involvement was seen in only two patients (3.6%), whereas approximately half of the patients with other histologic types had lymph node involvement in both the pulmonary hilum and mediastinum. Accordingly, the postsurgical stage of TC was stage I in more than 90% of the patients. However, approximately half of the patients with the other types of tumors were categorized as stage I, and there was no remarkable difference in the stage distribution between the different histologic types.

Prognosis

The follow-up for the patients in this study ranged from 2 to 197 months. The median follow-up time was 60 months. There were 124 tumor recurrences (39.0%) among all of the patients with NE tumors (Table 7). Compared with carcinoid tumors, high-grade NE tumors had a higher recurrence rate, at appproximately 50%. The survival curves for the 318 patients with NE tumors according to the histologic type are shown in Figure 1. The 5-year survival rates for patients with TC, AC, LCNEC, and SCLC were 96.2%, 77.8%, 40.3%, and 35.7%, respectively. The histologic type as NE tumor significantly affected the prognosis of the patients ($P = .0001$). The prognosis of AC was significantly better than the prognosis of both LCNEC and SCLC ($P = .0406$), which means that intermediate-grade malignancy (AC) could be differentiated from high-grade malignancy (LCNEC and SCLC). The survival curves of LCNEC and SCLC were superimposed, and there was no difference in survival ($P = .9147$). Survival was further analyzed within the same stage category, and a range of prognoses was seen. The relative grade of malignancy was reproduced within each stage category; in stage I patients (n = 175), the 5-year survival rates for TC, AC, LCNEC, and SCLC were 98.0%, 75.0%, 57.8%, and 42.2%, respectively (Fig 2). Again, there was no survival difference between LCNEC and SCLC ($P = .1851$), although the 5-year survival rate was numerically better for LCNEC. In stage II patients (n = 46), the 5-year survival rates for TC, AC, LCNEC, and SCLC were 75.0%, 100%, 31.9%, and 38.9%, respectively. In the multivariate analyses, the following variables were entered based on the results of univariate analyses: histologic type, symptoms, completeness of resection, nodal status, pathologic stage, and age. Among these variables, a histologic type of high-grade NE tumor was the most significant prognostic factor, with risk ratios (RRs) for SCLC and LCNEC of 17.40 and 17.69, respectively. Other significant prognostic factors included incomplete resection (RR = 3.13), symptoms (RR = 1.69), nodal involvement (RR = 2.23), and old age (RR = 1.53).

Table 3. Details of Histologic Diagnosis of SCLC

Histologic Type	No. of Patients	%
SCLC, not combined	83	73.4
SCLC, combined	30	26.6
With LCNEC	15	13.3
With AD	9	8.0
With SQ	5	4.4
With AD + SQ	1	0.9
Total	113	100

Abbreviations: LCNEC, large-cell neuroendocrine carcinoma; SCLC, small-cell lung carcinoma; AD, adenocarcinoma; SQ, squamous-cell carcinoma.

Table 4. Clinicopathologic Profiles According to the Histologic Type

Profile	Histologic Type TC (n = 55)	AC (n = 9)	LCNEC (n = 141)	SCLC (n = 113)	Total (N = 318)
Age, years					
Median	52	63	66	67	65
Range	17-83	38-73	38-88	40-84	17-88
Sex					
Female, No.	23	5	15	23	66
Male					
No.	32	4	126	90	252
%	58.2	44.4	89.4	79.7	79.3
Paraneoplastic syndrome					
No.	1	0	0	3	4
%	1.8	0	0	2.7	1.3
Present and past smokers					
No.	30	5	139	106	280
%	54.6	55.6	98.6	93.8	88.1

Abbreviations: TC, typical carcinoid; AC, atypical carcinoid; LCNEC, large-cell neuroendocrine carcinoma; SCLC, small-cell lung carcinoma.

DISCUSSION

A population of NE cells can be recognized in the normal bronchoalveolar structures in the lung, where NE defines specific cellular characteristics and the ability to uptake and decarboxylate amine precursors.[1] These features are reflected by the morphology, such as

Table 5. Percentage of Abnormal Elevations of the Tumor Markers CEA, NSE, and proGRP

	Histologic Type											
	TC (n = 55)			AC (n = 9)			LCNEC (n = 141)			SCLC (n = 113)		
Tumor Marker	%	No. of Patients With Abnormally Elevated Serum Level	No. of Patients Measured	%	No. of Patients With Abnormally Elevated Serum Level	No. of Patients Measured	%	No. of Patients With Abnormally Elevated Serum Level	No. of Patients Measured	%	No. of Patients With Abnormally Elevated Serum Level	No. of Patients Measured
CEA	5.9	3	51	11.1	1	9	48.5	63	130	40.7	44	108
NSE	0	0	42	0	0	5	12.4	13	105	2.3	2	88
proGRP	7.1	1	14	100	1	1	25.8	8	29	48.5	16	31

Abbreviations: TC, typical carcinoid; AC, atypical carcinoid; LCNEC, large-cell neuroendocrine carcinoma; SCLC, small-cell lung carcinoma; LCC, large-cell carcinoma; CEA, carcinoembryonic antigen; NSE, neuron-specific enolase; proGRP, progastrin-releasing peptide.

secretory granules and dense core granules by electron microscopy. However, the clinical implications of these NE characteristics (NE phenotype and NE morphology) in lung tumors have not yet been defined, especially in relation to the proper choice of treatment strategy. For SCLC, which shows a chemosensitive and aggressive nature, a standard therapeutic strategy has been established apart from other histologies. However, other NE tumors require the further refinement of histology-specific treatment.

NE lung tumors exhibit a spectrum of histologies, clinical profiles, and biologic behaviors ranging from relatively indolent TC to histologically high-grade, biologically aggressive tumors.[2-5] The grading was proposed in the 1999 WHO classification, with rigorous criteria for each subtype, even though LCNEC is still considered a variant form of large-cell carcinoma.[14] According to the WHO classification, AC can be differentiated from TC by a higher mitotic activity and/or the presence of necrosis. Although LCNEC is characterized by the NE morphology (nesting, palisading, and rosettes), a high mitotic rate, necrosis, cytologic features similar to non–small-cell lung cancer, and positive immunohistochemical staining for NE markers, it can sometimes be difficult to differentiate between LCNEC and SCLC. Even for an expert pathologist, the cytologic features falling between LCNEC and SCLC can make it difficult to define the histology as either SCLC or LCNEC, as seen in 14 tumors in the present series. One of the issues in the present WHO classification is that, despite the morphologic and clinical close relationship between SCLC and LCNEC, these tumors are placed in different categories. Specifically, LCNEC is recognized as a part of non–small-cell carcinoma, and the present therapeutic strategy is being planned in a histology-specific basis as SCLC or non-SCLC. Further assessment of therapeutic response is a high-priority issue, which will also justify the distinction between LCNEC and SCLC.

The most significant clinical and pathologic implication of the present study is the determination of the relative grade of malignancy of each histologic type among NE tumors. In particular, for the three

Table 6. Pathologic Profiles According to the Histologic Type

	Histologic Type									
	TC (n = 55)		AC (n = 9)		LCNEC* (n = 141)		SCLC (n = 113)		Total (N = 318)	
Profile	No. of Patients	%	No. of Patients	%	No. of Patients	%	No. of Patients	%	No. of Patients	%
Tumor diameter, mm										
Mean	26		26		41		29		34	
Range	9-70		13-44		7-140		7-75		7-140	
Postsurgical stage										
I	50	90.9	4	44.4	63	45.3	58	51.3	175	55.4
II	4	7.3	2	22.2	22	15.9	18	16.0	46	14.6
IIIA	1	1.8	2	22.2	32	23.0	24	21.2	59	18.7
IIIB	0	0	0	0	13	9.4	12	10.6	25	7.9
IV	0	0	1	11.1	9	6.5	1	0.9	11	3.5
Nodal involvement										
N0	53	96.4	5	55.6	76	55.1	65	57.5	199	63.2
N1	1	1.8	2	22.2	26	18.8	23	20.4	52	16.5
N2	1	1.8	2	22.2	33	23.9	24	21.2	60	19.1
N3	0	0.0	0	0.0	3	2.2	1	0.9	4	1.3

Abbreviations: TC, typical carcinoid; AC, atypical carcinoid; LCNEC, large-cell neuroendocrine carcinoma; SCLC, small-cell lung carcinoma.
*Data on the stage and nodal status were not available in two and three patients with LCNEC, respectively.

Table 7. Outcome of Patients With NE Tumors

Outcome	Histologic Type: TC (n = 55) No. of Patients	%	AC (n = 9) No. of Patients	%	LCNEC (n = 141) No. of Patients	%	SCLC (n = 113) No. of Patients	%	Total (N = 318) No. of Patients	%
Tumor recurrence	2	3.6	3	33.3	68	48.2	54	47.8	124	39.0
Locoregional	1		1		17		10		30	
Distant	1		2		34		18		55	
Both	0		0		16		16		36	
Unknown	0		0		1		1		4	
All deaths	3	5.5	2	22.2	84	59.6	69	61.1	158	49.7
Cancer death	1	33.3	0	0.0	62	73.8	43	63.2	106	67.5

Abbreviations: TC, typical carcinoid; AC, atypical carcinoid; LCNEC, large-cell neuroendocrine carcinoma; SCLC, small-cell lung carcinoma; NE, neuroendocrine.

histologic types that are considered intermediate- or high-grade malignancy (AC, LCNEC, and SCLC), the present findings clearly revealed their relative prognoses. There have been several previous reports on the prognosis of NE tumors of the lung. However, relatively few cases of high-grade NE tumors have been included. On the basis of their own diagnostic criteria, Travis et al[5] reported that the 5-year survival rates for TC, AC, LCNEC, and SCLC were 87%, 56%, 27%, and 9%, respectively. Garcia-Yuste et al[4] reported that the 5-year survival rates for TC, AC, LCNEC, and SCLC were 96%, 72%, 21%, and 14%, respectively. Neither report described a significant difference in survival between LCNEC and SCLC. As for LCNEC, the reported 5-year survival rates have ranged from 13% to 47%.[4,6,9,11,12] The 5-year survival rate of LCNEC in our present series was 41.3%, which is within the range of the rates reported previously. Even for stage I disease, the reported 5-year survival rates have been approximately 10% to 30%.[4,6,9,12] In the present series, however, the 5-year survival rate of stage I LCNEC was 60%, which was higher than the rates in previous reports. However, considering the 5-year survival rate of stage I non–small-cell lung cancer, LCNEC is the histology with the worst prognosis among non–small-cell histologies.[15] Also, we confirmed that LCNEC shows almost the same prognosis as SCLC. These two histologies also shared similar clinicopathologic backgrounds, such as smoking history and sex.

In high-grade NE tumors, the existence of borderline cases between LCNEC and SCLC has been noted. In the process of central pathologic review of the present study, there were 14 borderline cases between LCNEC and SCLC, which required another session of panel meetings to reach the consensus regarding the histology as either LCNEC or SCLC. There might be three factors that are closely related to the difficulties in the diagnosis; these are technical issues in the preparation of specimens, diagnostic reproducibility issues, and diagnostic criteria issues. There are several technical issues that make the diagnosis difficult. One is the poor histology as a result of poor fixation, extensive tumor necrosis, and sections that are cut too thick or poorly staining, although the preparation of the slides was completely centralized in the present study to minimize these issues. The histologic heterogeneity with the different cellular sizes and different proportions also affects the diagnosis.[16] The fact that the cell size in SCLC tends to be larger in the large, well-fixed specimens should be well recognized.[17]

It has been well known for SCLC that expert lung cancer pathologists disagree about the diagnosis in approximately 5% to 6% of the

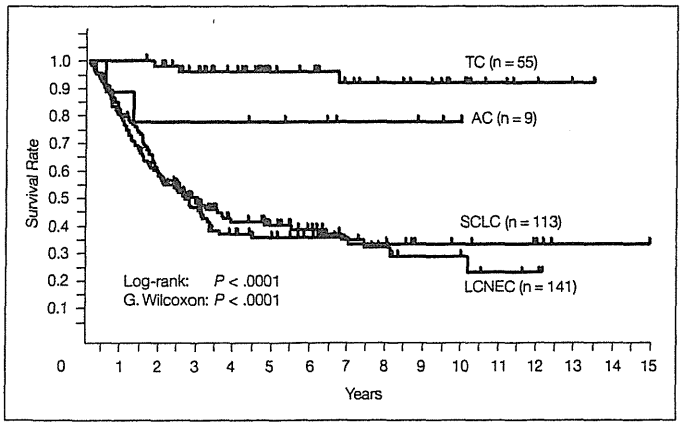

Fig 1. Overall survival curves in neuroendocrine tumors of all stages (N = 318) according to the following histologic types: TC, typical carcinoid (n = 55); AC, atypical carcinoid (n = 9); LCNEC, large-cell neuroendocrine carcinoma (n = 141); and SCLC, small-cell lung carcinoma (n = 113). The histologic type significantly affected the survival ($P < .0001$, log-rank test).

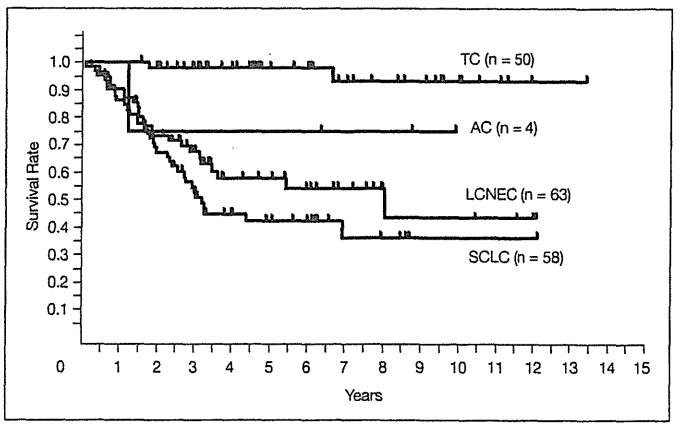

Fig 2. Overall survival curves in stage I neuroendocrine tumors (n = 175) according to the following histologic types: TC, typical carcinoid (n = 50); AC, atypical carcinoid (n = 4); LCNEC, large-cell neuroendocrine carcinoma (n = 63); and SCLC, small-cell lung carcinoma (n = 58). The histologic type significantly affected the survival ($P < .0001$, log-rank test).

cases.[18] In the present study, there was difficulty in the diagnosis of 14 tumors, which composed 5.5% of the 254 high-grade NE tumors; this percentage is quite similar to those previously reported. As part of the diagnostic criteria, the cellular and nuclear size is an important part in the differentiation between LCNEC and SCLC. According to the morphometric analysis by Marchevsky et al,[19] a considerable overlap of nuclear size was shown between LCNEC and SCLC, and the authors addressed that these two histologies should be merged as a single group of high-grade NE carcinoma. However, it is not clear how they could reach the definitive diagnosis as LCNEC or SCLC despite the overlapping cellular and nuclear size. These data, as well as our own, demonstrate that the cell size alone is insufficient as a criterion for establishing the diagnosis of high-grade NE tumors, and a constellation of criteria needs to be used. We still need more pathobiologic characteristics (and perhaps, they are more likely to be molecular rather than morphologic) to make the differentiation between SCLC and LCNEC clearer.

The limitations of this study must also be addressed. In this study, only surgical cases were collected to ensure that a thorough investigation of histopathologic features would be possible, and advanced, unresectable tumors were excluded. As is well known, most patients with SCLC are not candidates for resection because of local/systemic spread of the tumor. It is speculated that typical SCLC arises in the hilum and metastasizes to remote organs at a relatively early stage of the disease. In this sense, the resected SCLC in the present series may not represent typical SCLC, which might have a more aggressive nature. Although it will still be difficult to obtain enough specimens or to perform an immunohistochemical study using only biopsy samples in nonsurgical patients, future studies should include advanced diseases.

In conclusion, the present, large-scale, multi-institutional study defined the prognostic spectrum of pulmonary NE tumors as TC, AC, LCNEC, and SCLC, where LCNEC and SCLC were similarly aggressive. Future studies should clarify the histology-specific sensitivity to treatment, especially with regard to chemoradiotherapy. If similar responses are found, the histologic distinction at least has little significance in the planning of treatment strategy.

REFERENCES

1. Pearse AGE: The cytochemistry and ultrastructure of polypeptide hormone producing cells of the APUD series and the embryologic, physiologic and pathologic implications of the concept. J Histochem Cytochem 17:303-313, 1969
2. Travis WD, Linnoila RI, Tsokos MG, et al: Neuroendocrine tumors of the lung with proposed criteria for large-cell neuroendocrine carcinoma: An ultrastructural, immunohistochemical, and flow cytometric study of 35 cases. Am J Surg Pathol 15:529-553, 1991
3. Cooper WA, Thourani VH, Gal AA, et al: The surgical spectrum of pulmonary neuroendocrine neoplasms. Chest 119:14-18, 2001
4. Garcia-Yuste M, Matilla JM, Alvarez-Gago T, et al: Prognostic factors in neuroendocrine lung tumors: A Spanish multicenter study. Ann Thorac Surg 70:258-263, 2000
5. Travis WD, Rush W, Flieder DB, et al: Survival analysis of 200 pulmonary neuroendocrine tumors with clarification of criteria for atypical carcinoid and its separation from typical carcinoid. Am J Surg Pathol 22:934-944, 1998
6. Dresler CM, Ritter JH, Patterson GA, et al: Clinical-pathologic analysis of 40 patients with large cell neuroendocrine carcinoma of the lung. Ann Thorac Surg 63:180-185, 1997
7. Jiang SX, Kameya T, Shoji M, et al: Large cell neuroendocrine carcinoma of the lung: A histological and immunohistochemical study of 22 cases. Am J Surg Pathol 22:526-537, 1998
8. Iyoda A, Hiroshima K, Toyozaki T, et al: Clinical characterization of pulmonary large cell neuroendocrine carcinoma and large cell carcinoma with neuroendocrine morphology. Cancer 91:1992-2000, 2001
9. Takei H, Asamura H, Maeshima A, et al: Large cell neuroendocrine carcinoma of the lung: A clinicopathologic study of eighty-seven cases. J Thorac Cardiovasc Surg 124:285-292, 2002
10. Mazieres J, Daste G, Molinier L, et al: Large cell neuroendocrine carcinoma of the lung: Pathological study and clinical outcome of 18 resected cases. Lung Cancer 37:287-292, 2002
11. Zacharias J, Nicholson AG, Ladas GO, et al: Large cell neuroendocrine carcinoma and large cell carcinomas with neuroendocrine morphology of the lung: Prognosis after complete resection and systematic nodal dissection. Ann Thorac Surg 75:348-352, 2003
12. Paci M, Cavazza A, Annessi V, et al: Large cell neuroendocrine carcinoma of the lung: A 10-year clinicopathologic retrospective study. Ann Thorac Surg 77:1163-1167, 2004
13. Sobin LH, Wittekind C: International Union Against Cancer: TNM Classification of Malignant Tumors (ed 5). New York, NY, Wiley-Liss, 1997
14. Travis WD, Colby TV, Corrin B, et al: Histological typing of lung and pleural tumors, in World Health Organization International Histological Classification of Tumors. Berlin, Germany, Springer, 1999, pp 7-12
15. Naruke T, Kondo H, Tsuchiya R, et al: Prognosis and survival after resection for bronchogenic carcinoma based on the 1997 TNM-staging classification: The Japanese experience. Ann Thorac Surg 71:439-442, 2001
16. Vollmer RT: The effect of cell size on the pathologic diagnosis of small and large cell carcinomas of the lung. Cancer 50:1380-1383, 1982
17. Nicholson S, Beasley MB, Brambilla E, et al: Small cell lung carcinoma (SCLC): A clinicopathologic study of 100 cases with surgical specimens. Am J Surg Pathol 26:1184-1197, 2002
18. Roggli VL, Vollmer RT, Greenberg SD, et al: Lung cancer heterogeneity: A blinded and randomized study of 100 consecutive cases. Hum Pathol 16:569-579, 1985
19. Marchevsky AM, Gal AA, Shah S, et al: Morphometry confirms the presence of considerable nuclear size overlap between "small cells" and "large cells" in high-grade pulmonary neuroendocrine neoplasms. Am J Clin Pathol 116:466-472, 2001

Appendix

The Appendix is included in the full-text version of this article, available online at www.jco.org. It is not included in the PDF (via Adobe® Acrobat Reader®) version.

Authors' Disclosures of Potential Conflicts of Interest

The authors indicated no potential conflicts of interest.

Author Contributions

Conception and design: Hisao Asamura, Toru Kameya, Yoshihiro Matsuno, Masayuki Noguchi, Hirohito Tada, Yuichi Ishikawa, Tomoyuki Yokose, Shi-Xu Jiang, Takeshi Inoue, Ken Nakagawa, Kanji Nagai
Financial support: Hisao Asamura
Administrative support: Hisao Asamura
Provision of study materials or patients: Hisao Asamura, Toru Kameya, Yoshihiro Matsuno, Masayuki Noguchi, Hirohito Tada, Yuichi Ishikawa, Tomoyuki Yokose, Shi-Xu Jiang, Takeshi Inoue, Ken Nakagawa, Kanji Nagai
Collection and assembly of data: Hisao Asamura, Toru Kameya, Yoshihiro Matsuno, Masayuki Noguchi, Hirohito Tada, Yuichi Ishikawa, Tomoyuki Yokose, Shi-Xu Jiang, Takeshi Inoue, Ken Nakagawa, Kinuko Tajima, Kanji Nagai
Data analysis and interpretation: Hisao Asamura, Toru Kameya, Yoshihiro Matsuno, Masayuki Noguchi, Hirohito Tada, Yuichi Ishikawa, Tomoyuki Yokose, Shi-Xu Jiang, Takeshi Inoue, Ken Nakagawa, Kinuko Tajima, Kanji Nagai
Manuscript writing: Hisao Asamura, Toru Kameya, Yoshihiro Matsuno, Masayuki Noguchi, Hirohito Tada, Yuichi Ishikawa, Tomoyuki Yokose, Shi-Xu Jiang, Takeshi Inoue, Ken Nakagawa, Kanji Nagai
Final approval of manuscript: Hisao Asamura

Int. J. Radiation Oncology Biol. Phys., Vol. 63, No. 5, pp. 1427–1431, 2005

0360-3016/05/$–see front matter

ELSEVIER

doi:10.1016/j.ijrobp.2005.05.034

CLINICAL INVESTIGATION **Lung**

CLINICAL OUTCOMES OF A PHASE I/II STUDY OF 48 Gy OF STEREOTACTIC BODY RADIOTHERAPY IN 4 FRACTIONS FOR PRIMARY LUNG CANCER USING A STEREOTACTIC BODY FRAME

YASUSHI NAGATA, M.D., PH.D., KENJI TAKAYAMA, M.D., YUKINORI MATSUO, M.D., YOSHIKI NORIHISA, M.D., TAKASHI MIZOWAKI, M.D., PH.D., TAKASHI SAKAMOTO, M.D., MASATO SAKAMOTO, M.D., MICHIHIDE MITSUMORI, M.D., PH.D., KEIKO SHIBUYA, M.D., NORIO ARAKI, M.D., SHINSUKE YANO, PH.D., AND MASAHIRO HIRAOKA, M.D., PH.D.

Department of Therapeutic Radiology and Oncology, Kyoto University, Graduate School of Medicine, Sakyo, Kyoto, Japan

Purpose: To evaluate the clinical outcomes of 48 Gy of three-dimensional stereotactic radiotherapy in four fractions for treating Stage I lung cancer using a stereotactic body frame.

Methods and Materials: Forty-five patients who were treated between September 1998 and February 2004 were included in this study. Thirty-two patients had Stage IA lung cancer, and the other 13 had Stage IB lung cancer where tumor size was less than 4 cm in diameter. Three-dimensional treatment planning using 6–10 noncoplanar beams was performed to maintain the target dose homogeneity and to decrease the irradiated lung volume >20 Gy. All patients were irradiated using a stereotactic body frame and received four single 12 Gy high doses of radiation at the isocenter over 5–13 (median = 12) days.

Results: Seven tumors (16%) completely disappeared after treatment (CR) and 38 tumors (84%) decreased in size by 30% or more (PR). Therefore, all tumors showed local response. During the follow-up of 6–71 (median = 30) months, no pulmonary complications greater than an National Cancer Institute-Common Toxicity Criteria of Grade 3 were noted. No other vascular, cardiac, esophageal, or neurologic toxicities were encountered. Forty-four (98%) of 45 tumors were locally controlled during the follow-up period. However, regional recurrences and distant metastases occurred in 3 and 5 of T1 patients and zero and 4 of T2 patients, respectively. For Stage IA lung cancer, the disease-free survival and overall survival rates after 1 and 3 years were 80% and 72%, and 92% and 83%, respectively, whereas for Stage IB lung cancer, the disease-free survival and overall survival rates were 92% and 71%, and 82% and 72%, respectively.

Conclusion: Forty-eight Gy of 3D stereotactic radiotherapy in 4 fractions using a stereotactic body frame is useful for the treatment of Stage I lung tumors. © **2005 Elsevier Inc.**

Stereotactic body radiotherapy, Conformal radiotherapy, Lung cancer, Stereotactic body frame, Stereotactic radiotherapy.

INTRODUCTION

Stereotactic radiotherapy (SRT) for extracranial tumors has been recently performed to treat primary and secondary lung cancer and has subsequently been named stereotactic body radiotherapy. The advantages of hypofractionated radiotherapy for treating lung tumors are a shortened treatment course that requires fewer trips to the clinic than a conventional program and the adoption of a smaller irradiated volume allowed by greater setup precision. The disadvantages are uncertain effects of altered fractionation and the theoretical risk of worsening the ratio of normal tissue to tumor tissue through the use of a high dose per fraction. We previously published our setup accuracy (1), initial clinical results (2), computed tomography (CT) change after SRT (3), positron emission tomography (PET) evaluation after SRT (4) and treatment planning for SRT (5). In this study, the clinical results of lung cancer on our initial 5 years' worth of experiences are evaluated.

METHODS AND MATERIALS

Stereotactic radiotherapy was started for patients with lung tumor in July 1998 at Kyoto University. An integrated radiother-

Reprint requests to: Yasushi Nagata, M.D., Dept. of Therapeutic Radiology and Oncology, Kyoto University, Graduate School of Medicine, Sakyo, Kyoto, 606-8507, Japan. Tel: (+81) 75-751-3762; Fax: (+81) 75-751-3418; E-mail: nag@kuhp.kyoto-u.ac.jp

This work was partly presented at the 46th Annual Meeting of American Society for Therapeutic Radiology and Oncology (ASTRO), October 3–7, 2004, Atlanta, GA.

Supported by Grants-in-Aid No. 13470183, and 16390336 from the Ministry of Education and Science and No. 23765293 from the Ministry of Health, Welfare, and Labor in Japan.

Acknowledgments—The authors gratefully acknowledge Mr. Daniel Mrozek for his editorial assistance.

Received Feb 1, 2005, and in revised form May 20, 2005. Accepted for publication May 21, 2005.

apy system, including a CT simulator (CT-target, Shimadzu Corp., Kyoto, Japan), a three-dimensional (3D) radiotherapy treatment planning (RTP) machine (CADPLAN Ver 3.1, ECLIPSE Ver 7.1, Varian Associates, Palo Alto, CA), and a linear accelerator (CLINAC 2300C/D, Varian Associates) were in clinical use, and, in 1998, a stereotactic body frame (Stereotactic Body Frame, Elekta Corp., Stockholm, Sweden) was introduced for stereotactic body radiotherapy (SBRT).

Patients were fixed in the stereotactic frame (6, 7) using a vacuum pillow, and thereafter, six points were marked on the anterior chest wall with a laser marker and Indian ink. Then, respiratory movement of the tumor was observed with an X-ray simulator, where it was regulated when it was larger than 8 mm in the craniocaudal direction. A device called a diaphragm control, which is a board that pushes against the epigastric abdominal wall, was used for respiratory control. Serial CT scanning with 1 to 3 mm intervals around the tumor was performed over 4 s per slice without using the breath-hold technique. After the patient left the room, the target outlines of internal target volume (ITV) were drawn using the RTP machine. Our CT images included the respiratory movement of the target. Therefore, ITV including internal margins with clinical target volume (CTV) was delineated. ITVs and CTVs were not edited for anatomy. The setup margins between ITV and planning target volume (PTV) were 5 mm for the anteroposterior, 5 mm for the lateral, and 8–10 mm for the craniocaudal directions. Selection of the optimal direction of noncoplanar beams or dynamic arcs was performed by three experienced oncologists and technologists with the goal of the RTP being 6 to 10 portals for noncoplanar static beams. The beam energy used was 6 MV and the isocenter was single for all beams. All patients received four single treatments with 12 Gy of radiation prescribed at the isocenter. The mean ITV volume was 13 mL. The target dose homogeneity of ITV was within 20%, and the irradiated lung volume for >20 Gy (V20) was made as small as possible. As a result, the minimal and maximal ITV dose per fraction was 92% and 102.6%, respectively. The V20 ranged from 0.3% to 11.6% with a mean value of 4.3%. The irradiated dose–volume histograms of the other organs at risk, including the spinal cord, pulmonary artery, bronchus, and heart were also calculated. As a result, the mean and maximal single dose per fraction was 0.5 and 1.9 Gy for esophagus, 0.8 and 1.8 Gy for bronchus, 0.8 and 2.6 Gy for pulmonary artery, 0.3 and 2.7 Gy for heart, and 0.1 and 0.5 Gy for spinal cord, respectively (5). The target reference point dose was defined at the isocenter of the beam.

Before each treatment, anteroposterior and lateral portal films were taken for verification. The position of each patient was verified by three experienced oncologists and technologists at each treatment time. When the setup error was larger than 2 mm between the X-ray simulation film and portal film in any direction, the patient was repositioned and portal films were taken and verified again. Fractionated radiotherapy was performed with 4 days of 12 Gy over 5 to 13 (median = 12) days.

Using a linear-quadratic model (8), the biologic effective dose (BED) was here defined to be $nd\ (1+d/\alpha - \beta)$ Gy, where n is the fractionation number, d is the daily dose, and the α-β ratio was assumed to be 10 for tumors. The value was 105.6 Gy-BED for 48 Gy in four fractions (our study).

Forty-five patients with histologically confirmed Stage I primary lung cancer were treated between September 1998 and February 2004. Of them, 32 patients were Stage IA (T1N0M0); the other 13 were Stage IB (T2N0M0). Thirty-three patients were males and 12 were females, respectively. Their ages ranged between 51 and 87 years, and 77 years was the median for Stage IA, whereas they ranged between 68 and 80 years with 73 years as the median for Stage IB. Sixteen Stage IA patients were inoperable and the other 16 were operable but refused surgery, whereas 11 of the Stage IB patients were inoperable and the other 2 refused surgery. The histologies of the Stage IA patients were 16 squamous cell carcinoma, 15 adenocarcinoma, and 1 non–small-cell cancer and the Stage IB histologies were 8 squamous cell carcinoma and 5 adenocarcinoma.

The follow-up period was 6 to 71 (median = 30) months for the Stage IA patients and 6 to 61 (median = 22) months for Stage IB patients.

The eligibility criteria for the patients for Stage I primary lung cancer were *(1)* surgery was contraindicated or refused, *(2)* the patient could remain stable in the body frame for longer than 30 min (World Health Organization performance status ≤2), *(3)* oxygen was not required under normal conditions, *(4)* no active interstitial pneumonitis, and *(5)* written informed consent was obtained.

All patients were staged by bronchoscopy, CT, and after 1999 18-fluoro-deoxy-glucose (FDG)-PET scanning. The initial CT-based stage was changed in 2 patients with FDG-PET. For follow-up after the SRT, chest films were taken every month, and CT films were taken every 2 to 4 months for the first year and every 6 months between 1 year and 5 years after treatment. Toxicity was evaluated using the National Cancer Institute-Common Toxicity Criteria (NCI-CTC) Version 2.0.

Local tumor response was evaluated using the Response Evaluation Criteria in Solid Tumors criteria (9). Differentiation between radiation pneumonitis and residual tumor is difficult. However, new irregular densities which appeared within radiation field 2 to 6 months after radiotherapy and were thereafter reduced in size were considered to be radiation pneumonitis. All cases whose tumors decreased in size by 30% or more after radiotherapy were classified as PR. The cumulative survival rates were calculated using the Kaplan-Meier method.

RESULTS

Local tumor response

Of the 45 tumors, 7 (6 T1, 1 T2) (16%) completely disappeared after treatment (CR) and 38 (84%) decreased in size by 30% or more (PR). Also, all tumors showed a local response, but the distinction between tumor control from therapeutic effect was difficult. We considered any residual density surrounding a tumor after radiotherapy to be PR, and therefore the pathologic CR rate may have been much higher than 16%. During the follow-up, only one local failure that may be considered either marginal failure or regional nodal failure was encountered at 24 months, as shown in Fig. 1.

Toxicities

No severe symptomatic pulmonary complications (NCI-CTC Grade 3 or larger) were encountered. However, 2 patients (4%)—1 with T1 and the other with T2—received steroids after symptomatic pneumonitis and were categorized as NCI-CTC Grade 2. CT exams every 2 to 4 months after SRT showed mild pulmonary CT changes (NCI-CTC Grade 1) in the other 43 (96%) cases. Symptoms such as a

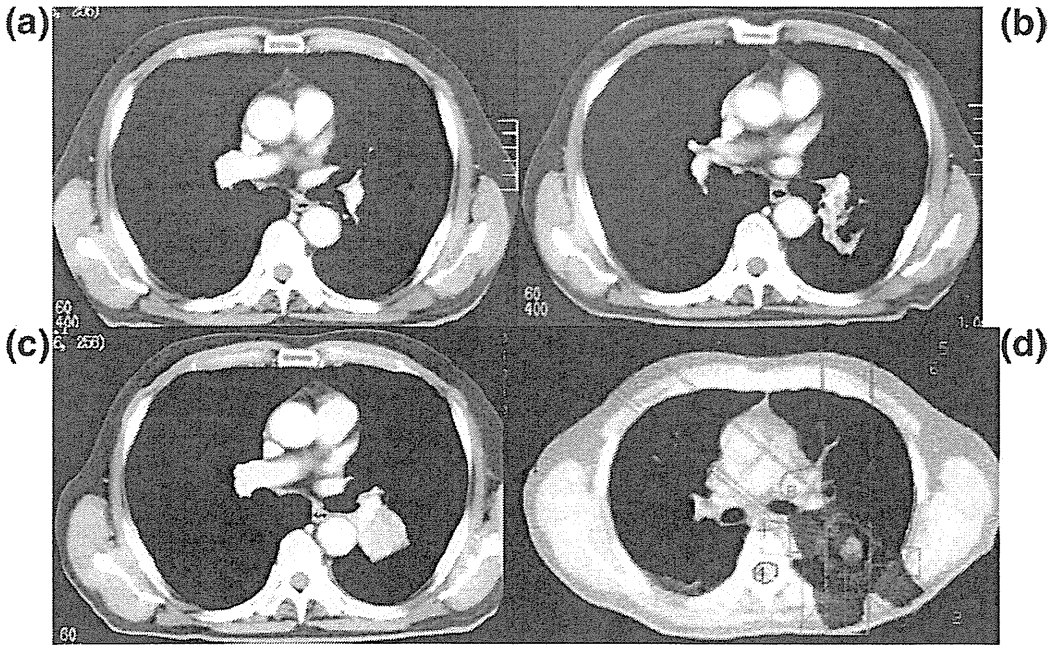

Fig. 1. A case of T1N0M0 lung cancer showing recurrence after stereotactic radiotherapy (SRT). The computed tomography images at 7 months (b, upper right) after SRT demonstrated a new soft-tissue density as well as radiation-induced lung damage (RILD) in the marginal area of the SRT that could not be observed at 2 months (a, upper left) after SRT. Initially, the density was considered to be RILD. However, the density increased in size at 16 months (c, lower left). The tumor was finally diagnosed as a local failure from either marginal failure or regional lymph nodal failure. The dose distributions are also shown (d, lower right).

mild cough, general malaise, and slight fever were present in 10 patients (22%) and were relieved without steroids at the outpatient clinic. A CT change in the liver was temporarily observed with the transient elevation of liver enzymes in a patient with a tumor in the right lower lung. As a result, no vascular complications, cardiac complications, esophageal complications, or neurologic complications were encountered.

Survival

T1N0M0 (Stage IA) primary lung cancer. For the 32 patients with histologically confirmed T1N0M0 Stage IA primary lung cancer, all but one of the tumors were locally controlled during the follow-up period. In 1 patient, a tumor locally recurred 24 months after SRT. In 3 patients, cancer recurred in regional hilar or mediastinal lymph nodes after 6, 12, and 24 months; in 4 patients, lung metastases after 2, 3, 20, and 55 months; and in the remaining patient, bone metastases were noted after 15 months without local recurrence. One patient died during the follow-up period from intercurrent causes.

Thus, the 1-year and 5-year local relapse-free survival rates were 100% and 95% as shown in Fig. 2. The disease-free survival rates after 1, 2, 3, and 5 years were 80%, 72%, 72%, and 72%, respectively, and the overall survival rates were 93%, 90%, 83%, and 83%, respectively.

T2N0M0 (Stage IB) primary lung cancer. Of the 13 patients with T2N0M0 Stage IB primary lung cancer, all tumors were locally controlled during the follow-up period. In 2 patients, cancer recurred distantly in the lung after 7 and 52 months, in 1 patient brain metastasis occurred after 10 months, and in the remaining patient liver metastases was noted after 12 months without local recurrence. Two patients died during the follow-up period from intercurrent causes.

Thus the 1- to 5-year local relapse free survival rates were also 100%. The disease-free survival after 1, 2, 3, and 5 years were 92%, 71%, 71%, and 71%, respectively, and the overall survival rates were 82%, 72%, 72%, and 72%, respectively, as shown in Fig. 3.

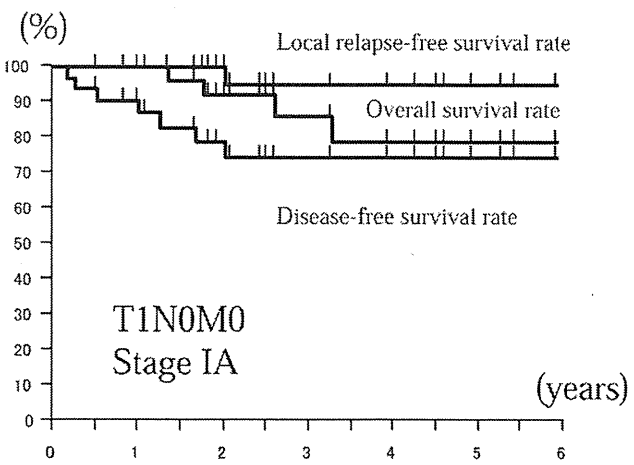

Fig. 2. The overall, local relapse-free, and overall disease-free survival rates of the patients with Stage IA (T1N0M0) lung cancer.

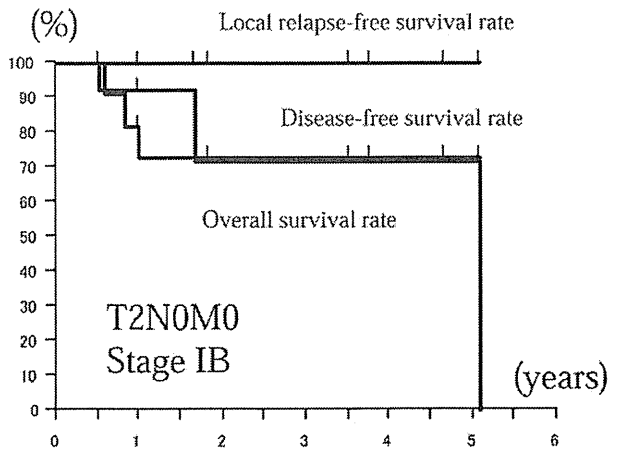

Fig. 3. The overall, local relapse-free, and overall disease-free survival rates of the patients with Stage IB (T2N0M0) lung cancer.

DISCUSSION

Local control rates of primary lung cancer with SRT has been previously reported by several authors: 94% (47/50) for 50 to 60 Gy in five fractions with a median follow-up of 36 months (10), 92% (22/24) for 60 Gy in eight fractions with a median follow-up of 24 months (11), 87% (30/37) for 60 Gy in three fractions with a median follow-up of 15 months (12), 85% for 48 to 60 Gy in eight fractions with a median follow-up of 17 months (13), 95% for 45 to 56.2 Gy in three fractions with a median follow-up of 10 months (14), and 97% (44/45) for 48 Gy in four fractions with a median follow-up of 22 to 30 months (as shown in Table 1 in this study). Using a linear-quadratic model with an α-β ratio = 10, our fractionation of 12 Gy × 4 was equal to 2 Gy × 44 = 88 Gy. A BED larger than 100 Gy may be effective for STI of solitary lung cancer with a local control rate of more than 85%. Timmerman (12) concluded that a 60 Gy marginal dose in three fractions is the limiting dose. Considering our clinical results, a further dose escalation study of more than 48 Gy in four fractions is not necessary for tumors smaller than 4 cm in diameter.

The current standard choice for Stage IA lung cancer treatment is lobectomy (15). However, for many patients this is not indicated because of accompanying diseases, such as chronic obstructive pulmonary disease, cardiac disease, and diabetes. For them, various minimal surgical techniques are indicated, including wedge resection and video-assisted thoracoscopic surgery as well as ablation. The local control rates of various other modalities for primary Stage I lung cancer previously reported was 93% for wedge resection and 83–95% for VATS and the 5-year survival rates were 82% and 50–70%, respectively (16).

Onishi (17) recently reported results for 13 institutions in Japan, where they summarized 245 patients, 155 with Stage IA lung cancer and 90 with Stage IB lung cancer. The operable and inoperable patients totalled 87 and 158, respectively, and their results showed that the intercurrent death rate was especially high in the inoperable patient group. Moreover, the 5-year survival rates of operable patients irradiated with more than BED = 100 Gy was 90% for Stage IA and 84% for Stage IB, and their clinical results were as good as those for surgery.

During our follow-up, no serious complications were encountered, and only mild radiation pneumonitis (NCI-CTC Grade 2 or less) was detected by CT. Graham (18) reported that the tolerance of the pulmonary dose >20 Gy (V20) is 25% of the whole lung with low risk. Our >20 Gy irradiated volume (V20) of the whole lung was 1.0% to 11.6% (average = 4.5%), which was markedly smaller than that in their report. However, the V20 of the standard fraction with 2 Gy and that of the SRT with 12 Gy must be different. Further close follow-up is required. Another concern of our study was the effects on the central bronchus, pulmonary artery, esophagus, heart, and spinal cord. The effects of the hypofractionated dose on the main bronchus, pulmonary artery, heart, and esophagus have not been followed for a long enough time. For our clinical experiences thus far, no severe complications have been encountered. However, lethal pulmonary bleeding and esophageal ulcer have been previously reported by other institutions (19). A case with a skin ulcer that finally caused thoracocutaneous fistula and another case with acute cholecystitis due to abdominal press were reported in Japan. Therefore, long-term follow up is still necessary.

Considering the tumor control dose, after dose escalation from 40 Gy to 48 Gy, only one local recurrence was encountered for primary lung cancer, and no severe complications were encountered for all tumors. Therefore, we will continue this schedule for the treatment of primary lung cancer. Systemic chemotherapy may be considered when the local tumor is well controlled and regional/distant metastases are frequent. On the other hand, the underlying pulmonary diseases could be a limiting factor for SRT of a solitary lung tumor. However, this should be discussed for each case. In our cases, 1 patient who had severe interstitial pneumonitis died of progression of pneumonitis 6 months after SRT. Because the occurrence of this pneumonitis was far distant from the irradiated tumor in the opposite lung, death was considered to be unrelated to the treatment. However, the effect of the scattered radiation dose cannot be completely neglected and the indications of SRT for the patients with interstitial pneumonitis should be limited. Our current indications are that a patient does not require oxygen under normal conditions and has no active interstitial pneumonitis shadow on a chest X-ray film. If these requirements are satisfied, this treatment can be performed without serious complications.

Recently, we started a multi-institutional Phase II study for T1N0M0 non–small-cell lung cancer under Japan Clinical Oncology Group (http://www.jcog.jp/) number 0403. Sixteen institutions have entered together and started the same dose SBRT with 48 Gy at the isocenter in four fractions for T1N0M0 lung cancer. The results of SRT for inoperable and operable Stage I lung cancer patients are awaited.

Table 1. Clinical results of stereotactic radiotherapy for primary lung cancer

Author (year)	Total dose (Gy)	Daily dose (Gy)	Reference point	Local control	Median follow-up
Uematsu (2001)	50–60	10	80% margin	94% (47/50)	36 months
Arimoto (1998)	60	7.5	Isocenter	92% (22/24)	24 months
Timmerman (2003)	60	20	80% margin	87% (30/37)	15 months
Onimaru (2003)	48–60	6–7.5	Isocenter	80% (20/25)	17 months
Wulf (2004)	45–56.2	15–15.4	80% margin	95% (19/20)	10 months
This study (2005)	48	12	Isocenter	97% (44/45)	30 months

The primary indication for stereotactic radiotherapy in lung cancer could be a Stage Ia (T1N0M0) patient. Very early stage lung cancer can now be detected by screening CT examination, and these cases are also good indications for SRT. However, the issue of these cases is histologic confirmation. In our clinical experience, 7 of 95 total SRT cases could not be finally confirmed histologically. Of course, these seven cases are not included in this study. They could not be histologically confirmed because of the failure or difficulty in CT-guided biopsy or transbronchoscopic lung biopsy. CT screening has revealed very early staged lung cancer with ground glass opacity and some patients with severe emphysema could be contraindicated for biopsy. Therefore, the indication for SRT for these cases without histologic confirmation should be discussed in the future. When the tumor becomes larger than 3 cm in diameter, which corresponds to Stage Ib (T2N0M0), SRT is possible. However, the intratumor dose becomes less homogeneous, and the rate of occult distant metastases may increase. Therefore, the extension of the indication of this technique for T2 tumors requires more consideration for dose escalation or adjuvant chemotherapy.

CONCLUSION

The feasibility and accuracy of 3D conformal radiotherapy using a stereotactic body frame was evaluated. 3D SRT using a stereotactic body frame is a safe and effective treatment method for solitary lung tumors. Thus further clinical studies are warranted in future.

REFERENCES

1. Negoro Y, Nagata Y, Aoki T, *et al.* The effectiveness of an immobilization device in conformal radiotherapy for lung tumor: Reduction of respiratory tumor movement and evaluation of daily set-up accuracy. *Int J Radiat Oncol Biol Phys* 2001;50:889–898.
2. Nagata Y, Negoro Y, Aoki T, *et al.* Clinical outcomes of 3-D conformal hypofractionated single high dose radiotherapy for one or two lung tumors using a stereotactic body frame. *Int J Radiat Oncol Biol Phys* 52;1041–1046, 2002.
3. Aoki T, Nagata Y, Negoro Y, *et al.* Evaluation of CT appearance of lung injury after three-dimensional conformal stereotactic radiotherapy for solitary lung tumors. *Radiology* 2004; 230:101–108.
4. Ishimori T, Saga T, Nagata Y, *et al.* 18F-FDG and 11C-Methionine evaluation of the treatment response of lung cancer after stereotactic radiotherapy. *Ann Nuclear Med* 2004;18: 669–674.
5. Takayama K, Nagata Y, Negoro Y, *et al.* Treatment planning of stereotactic radiotherapy for solitary lung tumor. *Int J Radiat Oncol Biol Phys* 2005;61:1565–1571.
6. Blomgren H, Lax I, Goeranson H, *et al.* Radiosurgery for tumors in the body: Clinical experience using a new method. *J Radiosurg* 1998;1:63–74.
7. Lax I, Blomgren H, Larson D, *et al.* Extracranial stereotactic radiosurgery of localized target. *J Radiosurg* 1998;1:135–148.
8. Yaes RJ, Patel P, Maruyama Y. On using the linear-quadratic model in daily clinical practice. *Int J Radiat Oncol Biol Phys* 1991;20:1353–1362.
9. Therasse P, Arbuck SG, Eisenhauer EA, *et al.* New guidelines to evaluate the response to treatment in solid tumors. *J Natl Cancer Inst* 2000;92:205–216.
10. Uematsu M, Shioda A, Tahara K, *et al.* Computed tomography-guided frameless stereotactic radiotherapy for stage I non-small-cell lung cancer: A 5-year experience. *Int J Radiat Oncol Biol Phys* 2001;51:666–670.
11. Arimoto T, Usubuchi H, Matsuzawa T, *et al.* Small volume multiple non-coplanar arc radiotherapy for tumors of the lung, head, and neck and the abdominopelvic region. In: Lemke HU, editor. CAR '98 Computer assisted radiology and surgery. Tokyo: Elsevier; 1998. p. 257–261.
12. Timmerman R, Papiez L, McGarry R, *et al.* Extracranial stereotactic radioablation: Results of a phase I study in medically inoperable stage I non-small cell lung cancer. *Chest* 2003;124:1946–1955.
13. Onimaru R, Shirato H, Shimizu S, *et al.* Tolerance of organs at risk in small-volume, hypofractionated, image-guided radiotherapy for primary and metastatic lung cancers. *Int J Radiat Oncol Biol Phys* 2003;56:126–135.
14. Wulf J, Haedinger U, Oppitz U, *et al.* Stereotactic radiotherapy for primary lung cancer and pulmonary metastases: A noninvasive treatment approach in medically inoperable patients. *Int J Radiat Oncol Biol Phys* 2004;60:186–196.
15. Lung Cancer Study Group. Randomized trial of lobectomy versus limited resection for T1N0 non-small cell lung cancer. *Ann Thorac Surg* 1995;60:615–623.
16. Luketich JD, Ginsberg RJ. Limited resection versus lobectomy for stage I non-small cell lung cancer. In: Pass HI, Mitchell JB, Johnson DH, *et al.*, editors. Lung cancer: Principles and practice. Philadelphia: Lippincott-Raven; 1996. p. 561–566.
17. Onishi H, Araki T, Shirato H, *et al.* Stereotactic hypofractionated high-dose irradiation for stage I non-small cell lung carcinoma. *Cancer* 2004;101:1623–1631.
18. Graham MV. Predicting radiation response. *Int J Radiat Oncol Biol Phys* 1997;39:561–562.
19. Herfarth KK, Debus J, Lohr F, *et al.* Stereotactic single dose radiation treatment of tumors in the lung. *Radiology* 2000;217: 148.

Int. J. Radiation Oncology Biol. Phys., Vol. 61, No. 5, pp. 1565–1571, 2005

0360-3016/05/$–see front matter

ELSEVIER

doi:10.1016/j.ijrobp.2004.12.066

PHYSICS CONTRIBUTION

TREATMENT PLANNING OF STEREOTACTIC RADIOTHERAPY FOR SOLITARY LUNG TUMOR

KENJI TAKAYAMA, M.D., YASUSHI NAGATA, M.D., PH.D., YOSHIHARU NEGORO, M.D., TAKASHI MIZOWAKI, M.D., PH.D., TAKASHI SAKAMOTO, M.D., MASATO SAKAMOTO, M.D., TETSUYA AOKI, M.D., SHINSUKE YANO, PH.D., SACHIKO KOGA, R.T.T., AND MASAHIRO HIRAOKA, M.D., PH.D.

Department of Therapeutic Radiology and Oncology, Graduate School of Medicine, Kyoto University, Kyoto, Japan

Purpose: To analyze the stereotactic radiotherapy (SRT) plans in terms of internal target volume (ITV) and organs at risk (OARs).

Methods and Materials: Treatment planning and dose distributions were analyzed using dose–volume histograms (DVHs) of ITV and OARs in 37 patients, who were treated for a solitary lung tumor with SRT. The stereotactic body frame (SBF) was used for immobilization and accurate setup. Prescription dose was 48 Gy in four fractions at the isocenter.

Results: Use of SBF limits the extent of the noncoplanar beam directions to prevent a collision with the Linac gantry. DVH analyses showed that the homogeneity index, defined as the ratio of maximum and minimum dose to ITV, ranged from 1.03 to 1.25 (mean, 1.12). The volume irradiated with 20 Gy or more (V_{20}) of the lung ranged from 0.3 to 11.6% (mean, 4.4%) of the whole lung volume. The maximum dose to the other OARs ranged from 0 to 11.8 Gy (mean, 0.5–2.7) per fraction. No clinically significant complications were encountered.

Conclusions: Despite the limitation of the beam arrangement, a homogeneous target dose distribution, while avoiding high doses to normal tissues, was obtained. © 2005 Elsevier Inc.

Stereotactic radiotherapy, Lung tumor, Treatment planning, Dose–volume histogram, Normal tissue.

INTRODUCTION

Stereotactic radiotherapy (SRT) has recently been applied to patients with small lung tumors. Initial clinical results including ours were favorable, and local control rates around 90% have been reported (1–9).

Few reports, however, have been made about details of treatment planning—such as beam arrangement, dose distribution to the target, and tolerance dose of normal tissues. Regarding normal tissue, the use of a single high dose rather than a conventional dose in consideration of the biologic effect may increase the risk of complication. However, few cases with severe toxicity have been reported.

At Kyoto University, we have treated more than 80 patients with this method since July 1998, with the approval of our institutional review board and written informed consent provided by all patients. Our initial reports on daily setup accuracy and clinical results have already been published (5, 10). This article reports on our treatment planning procedures and results, especially in terms of doses to internal target volume (ITV) and organs at risk (OARs) using dose–volume histograms (DVHs) for the first half of cases.

METHODS AND MATERIALS

Treatment planning procedure

A stereotactic body frame (SBF) (Elekta AB, Stockholm, Sweden) was used as an immobilization device. We have previously reported the details of its use and its effect on daily setup accuracy and reduction of respiratory tumor motion (10).

The following describes the flow chart of our treatment planning procedures. First, the body of the patient was fixed by means of a vacuum pillow in SBF. The patient was set in the supine position with both arms raised using a T-shaped holding bar. The patient and SBF were set on the couch of an X-ray simulator to measure

Reprint requests to: Yasushi Nagata, M.D., Ph.D., Department of Therapeutic Radiology and Oncology, Graduate School of Medicine, Kyoto University, 54 Kawahara-cho, Shogoin, Sakyo-ku, Kyoto, 606-8507, Japan. Tel: (+81) 75-751-3418; Fax: (+81) 75-751-3418; E-mail: nag@kuhp.kyoto-u.ac.jp

Presented in part at the 6th International Stereotactic Radiosurgery Society Congress in Kyoto, Japan, June 22–26, 2003.

Supported by a grant-in-aid No.09255255, No.10153231, and No.13410183 of the Ministry of Education, Culture, Sports, Science and Technology, and No.23765293 of the Ministry of Health, Labor and Welfare in Japan.

Acknowledgments—The authors gratefully acknowledge Mr. Daniel Mrosek for his secretarial editorial assistance.

Received Mar 4, 2004, and in revised form Dec 7, 2004. Accepted for publication Dec 17, 2004.

tumor movement during free breathing using fluoroscopy. When the tumor moved more than 10 mm in the craniocaudal (C-C) direction, a small abdominal pressing plate called a "diaphragm control" was applied before computed tomography (CT) scanning, which suppresses the movement of the diaphragm and reduces tumor movement during respiration. CT images were then sequentially scanned from the neck to the upper abdomen with a CT simulator. The CT slice thickness and pitch were 1 to 3 mm each in the area of the tumor and 10 mm each in the other areas. Each CT slice was scanned with an acquisition time of 4 s to include the whole phase of one respiratory cycle. A series of CT images, therefore, included the tumor and its respiratory motion. The isocenter coordinate was defined using a three-dimensional radiation treatment planning system (3D RTPS) (CADPLAN R.6.0.8, Varian Associates, Palo Alto, CA). Anteroposterior (A-P) and lateral films for verification were then obtained using the X-ray simulator at a designated isocenter. Because the CT simulator and the X-ray simulator employed the same couch in our integrated system, the patient's position on verification films was the same as that on CT images in relation to SBF (10).

The outlines of the target were delineated on 3D RTPS using lung CT window settings (window width 2000 Hounsfield units (HU) and window level −700 HU, typically). A physician delineated both the solid area (tumor itself), which could be seen even using mediastinal CT window settings (window width 350 HU and window level 40 HU, typically), and the surrounding obscure area, which could be seen only under lung CT settings. The obscure area is important because it indicates either tumor microscopic invasion or respiratory tumor motion. This target volume corresponded to the ITV in International Commission on Radiation Units and Measurements Report 62. The outlines of gross tumor volume and clinical target volume were included in the ITV, and gross tumor volume and clinical target volume could not be delineated on the planning CT in our system because the CT images already included the internal motion. Spiculation and pleural indentation were included within the ITV. Neither mediastinal nor hilar lymph nodes were included within the ITV.

The physician also delineated the outline of the following OARs: lung, spinal cord (canal), pulmonary artery, heart, and esophagus. The outline of the lung included that of the target. The pulmonary artery, heart, and esophagus were delineated with each outer contour and included both the wall and content of each organ. The pulmonary artery was delineated from its origin to the pulmonary hila. The esophagus was delineated from the level of the sternal notch to the esophagocardial junction.

Treatment planning was performed using the 3D RTPS, and 5–10 noncoplanar static ports were selected. Edges of the multileaf collimator (MLC) were located 8–10 mm outside of the ITV in the C-C direction and 5 mm in the A-P and lateral directions. The distance in the C-C direction was larger than that in the other directions, because the former was set to compensate for an irregular respiratory motion which could not be included in the ITV using the CT scan with the acquisition time of 4 s. The prescribed dose was 12 Gy per fraction at the isocenter, and the total dose was 48 Gy with four fractions. The dose was delivered by a linear accelerator (CLINAC 2300 C/D, Varian medical systems) with 6-MV photons. Each MLC had a 1-cm leaf width at the isocenter. One of the planning goals was to maintain a dose homogeneity of ITV within 10%, which meant a dose to ITV ranging from 90% to 110% of the isocenter dose. Another goal was to maintain V_{20} (the volume irradiated with 20 Gy or more) of the bilateral lung at less than 25%. Beam arrangement was also selected to minimize doses to OARs. The use of the beam that passed directly through the spinal cord was avoided.

Beam arrangement

The applicable area of noncoplanar beam directions is more limited in SRT for extracranial tumors compared with intracranial tumors. There are three main causes: *(1)* risk of collision of the couch and the gantry; *(2)* blockade of the contralateral posterior beams by the supporting metal bar at the couch center; and *(3)* usage of the SBF that might cause the additional collision with the gantry. Figure 1 shows examples of the applicable gantry angle range that varies depending on the couch angle. We usually shift the position of the supporting couch and SBF in the lateral direction to avoid the metal bar on the center of the couch for a posterior beam, as shown in Fig. 2a. The figure shows the scheme of the couch and SBF shift from the foot-side view, in which the couch is shifted to the left side by 16.5 cm, and the SBF is shifted to the right side by 6.5 cm to put the center of the right-sided target on the isocenter. To find the applicable beam directions on the 3D RTPS more easily, we made diagrams that indicated applicable combinations of couch and gantry angles (11). Fig. 2b shows the diagram for the right-sided tumor. The area between an upper line and a lower line presents the applicable combination of the gantry and couch angles in each different isocenter height from the SBF base that determines the couch height. The diagrams were very useful in finding applicable beam directions at the time of treatment planning.

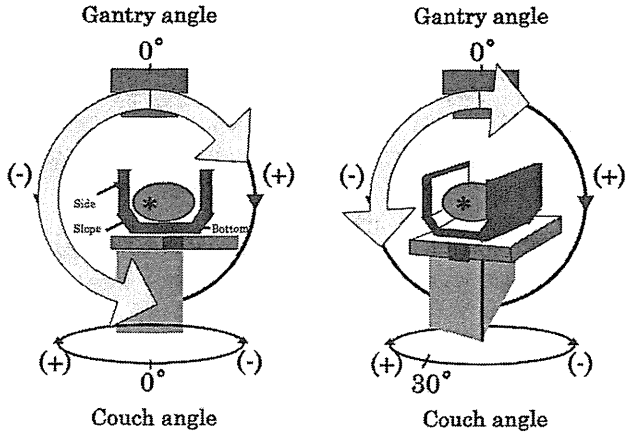

Fig. 1. Limitation of the couch and gantry angles. The left figure shows the applicable gantry position when the couch is set to the standard position (0° of the couch angle) and the tumor is in the right lung. The beam from the left direction cannot be used either because of the collision of the gantry and the couch or SBF. The beam from the posterior direction cannot be used either because of the interference of the supporting bar that lies in the center of the couch. Therefore, the applicable gantry angles are limited in the range of the thick arrow. Larger we set the couch rotation angle (e.g., 30° as shown in the right figure of Fig. 1), wider gets the zone in which the gantry and either the couch or stereotactic body frame mutually interfere. The range of the applicable gantry angle, therefore, is limited further as the thick arrow shows in the right figure. The supporting bar at the couch center is shown as a black square. The outer stiff frame of the stereotactic body frame consists of bilateral "side" walls, a "bottom" wall, and "slope" walls between the side and the bottom.

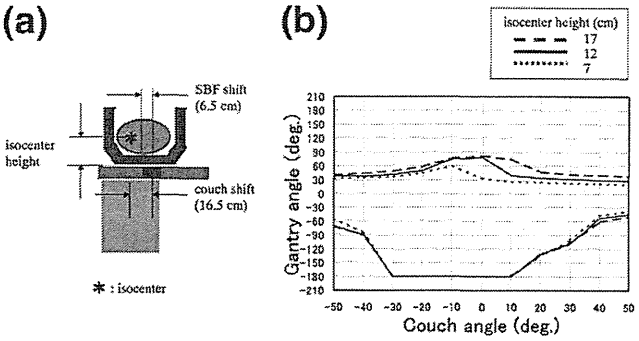

Fig. 2. Diagrams of beam arrangements. (a) Scheme of the couch and stereotactic body frame shift, which is necessary to avoid the metal bar on the center of the couch for a posterior beam. Isocenter height from the stereotactic body frame base is the parameter determining the couch height. (b) The applicable area of beam arrangement at the different isocenter heights. The area between each sequential line presents the applicable combination of the gantry and couch angles.

The procedure for choosing the optimal beam arrangement was forward planning based on our experiences. The beam arrangement used in our planning consisted of 5–10 beams, which included 1–4 coplanar beams and 2–6 noncoplanar beams. The alignment of the beams was chosen to be geometrically homogeneous wherever possible within the limitation. The use of opposing beams was avoided. The use of the beam that passed directly through the spinal cord was also avoided, although just one of the beams is allowed to pass directly through the spinal cord in recent planning. After checking the dose distribution by means of both DVH and dose distribution on axial images, modification of the beam alignment, number of beams, and weight of each beam was made to create an optimal dose distribution, which showed homogenous distribution to the target and low dose distribution to the normal tissues. A typical beam arrangement and the dose distribution are shown in Fig. 3 and Table 1.

Dose correction

There are two important issues for dose correction in SRT for lung tumors. One is lung inhomogeneity correction; the other is correction for dose attenuation caused by SBF.

We use the generalized Batho method to calculate the dose distribution with lung inhomogeneity correction. The center dose of lung tumors calculated by 3D RTPS without lung inhomogeneity correction were higher than the dose calculated with a house-made Monte Carlo simulation by 6% as an average (range 1–14%) in our institutional experiment. In contrast, the dose calculated with the generalized Batho method almost corresponded to the dose calculated with the Monte Carlo simulation. When the radiation field became too small, the dose calculated with the generalized Batho method did not correspond to the actual dose. Therefore, we did not use a radiation field smaller than 3 cm × 3 cm.

Another experiment revealed that the beams passing through the SBF showed a considerable dose reduction, although the frame, which has a honeycomb structure with a center of paper and surrounding glass fiber surface with edgings of pure birch, absorbs fewer X-rays compared with other materials. The outer stiff frame of the SBF consists of bilateral side walls, a bottom wall, and sloped walls between the side and bottom, as shown in Fig. 1. In the experiment, the mean dose attenuation ratio through each part of the frame was 7.5% for the side wall, 10.6% for the sloped wall, 9.5% for the bottom wall, 11.9% for transitional part between the side and sloped wall, and 11.8% for the transitional part between the sloped and bottom wall. The dose attenuation ratio ranged from 6.0 to 15.4%, and the mean value was 9.3%. Therefore, we used a uniform dose correction of 9.3% for beams passing through SBF in clinical use. According to another experiment using a phantom, the uniform dose correction of 9.3% minimized the dose difference from the actual dose by less than 3% (11).

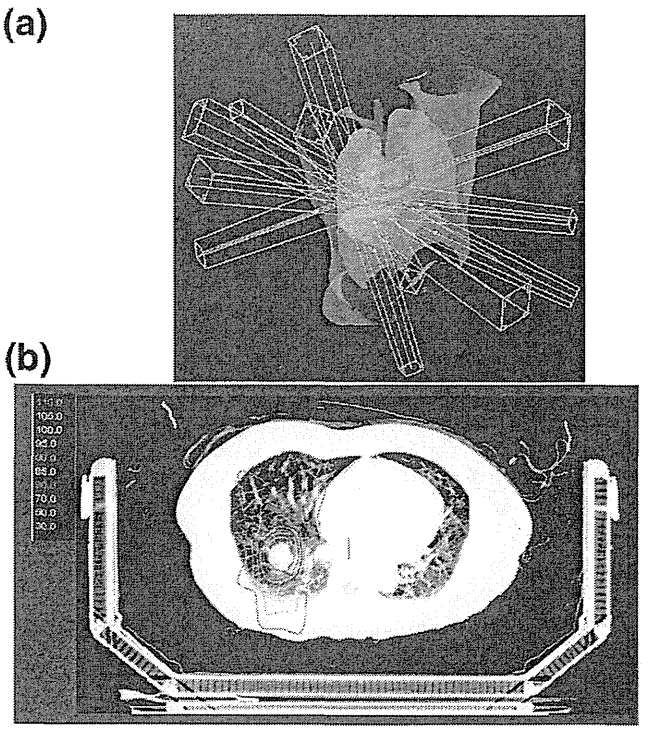

Fig. 3. A typical beam arrangement and the dose distribution. (a) A three-dimensional figure of a typical beam arrangement consisting of two coplanar beams and four noncoplanar beams. The detail of the gantry and the couch angles are shown in Table 1. (b) The two-dimensional dose distribution using this beam arrangement.

Analysis of treatment planning

We analyzed the plans of 37 consecutive patients who underwent hypofractionated single high-dose SRT for small lung tumors at our institute between October 1998 and December 2000. All tumors were located at periphery of the lung and were of sizes smaller than 4 cm in the largest diameter on a diag-

Table 1. A typical beam arrangement

Port no.	Gantry angle	Couch angle (degrees)
1	180	0
2	260	0
3	340	40
4	30	40
5	35	320
6	295	320

nostic CT image or radiograph. In the analysis of target dose, we evaluated maximum dose, minimum dose, 90% coverage volumes, and homogeneity index. Homogeneity index was defined as the ratio of maximum dose to minimum dose. In the analysis of dose to the lung, we evaluated the V_{20} as an index related to the risk of radiation pneumonitis. In the analysis of dose to the other normal tissues, we evaluated maximum dose and mean dose to the spinal cord, heart, esophagus, and pulmonary artery. The median (range) clinical follow-up was 32 (3–63) months.

RESULTS

Target dose

The ITV ranged from 0.3 to 41.3 mL (mean, 13.4 mL). The ITV maximum dose ranged from 100.0 to 107.5% (mean, 102.6%), and the ITV minimum dose ranged from 82.5 to 99.2% (mean, 92.0%). The homogeneity index ranged from 1.03 to 1.25 (mean, 1.12). Figure 4 shows the relationship of the target volume with minimum dose, maximum dose, and homogeneity index for all patients. The minimum dose generally decreased as the target volume increased (coefficient of determination: $r^2 = 0.53$). On the other hand, the homogeneity index increased as well, because the index nearly equaled to the inverse number of the minimum dose ($r^2 = 0.59$). When the ITV exceeded 30 mL, the minimum dose was less than 90% and the homogeneity index was more than 1.2 in all cases. The percentage of the target volume irradiated with a dose of 90% or more of the isocenter dose (90% coverage volumes) exceeded 99.5% in all patients but one, whose ITV exceeded 40 mL.

Dose to the normal tissues

Doses to the normal tissues were analyzed for the lung, spinal cord, esophagus, heart, pulmonary artery, and bronchus. The results are summarized in Table 2, except for the dose to the lung.

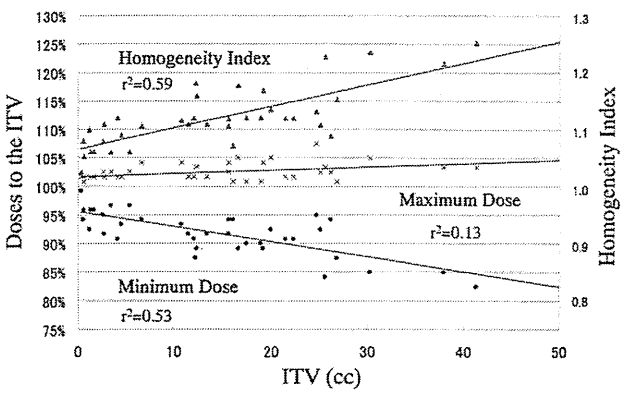

Fig. 4. Correlation with the internal target volume (ITV) and the dose to the ITV. Minimum and maximum doses to the ITV and homogeneity indices in each patient are presented in association with the value of ITV. Minimum dose had the tendency to decrease as the target volume increased ($r^2 = 0.53$). Homogeneity index had also a tendency to increase ($r^2 = 0.59$).

Table 2. Dose to the normal tissues

	Mean dose	Max dose
	Mean (range) Gy/fraction	
Esophagus	0.5 (0.0–1.3)	1.9 (0.1–5.2)
Bronchus	0.8 (0.0–5.0)	1.8 (0.1–7.9)
Pulmonary artery	0.8 (0.1–1.5)	2.6 (0.1–11.8)
Heart	0.3 (0.0–1.5)	2.7 (0.1–10.6)
Spinal cord	0.1 (0.0–0.2)	0.5 (0.0–2.2)

Mean and maximum doses of the normal tissues in each plan are summarized in this table. The values outside and between parentheses represent the average and the range for all patients, respectively.

Lung. V_{20} of the whole lung ranged from 0.3% to 11.6% with a mean value of 4.3%. There were 3 patients whose V_{20} exceeded 10%. One of them had only one lung because of tuberculosis. The other 2 patients had larger tumors than all other patients. Figure 5 shows the relationship of the target volume with V_{20} of the whole lung in all patients. In most of the patients, V_{20} increased in proportion to the target volume. Some patients, however, showed much larger V_{20} than patients with the same target volume when the tumor was located near the center of the lung. On the other hand, some patients showed smaller V_{20} when the tumor was located near the chest wall. Regarding pulmonary toxicity, only 2 patients (5%) had Grade 2 radiation pneumonitis in the National Cancer Institute - Common Toxicity Criteria (NCI-CTC), and no patients had more than Grade 2 pneumonitis. Thirty-four patients (92%) showed Grade 1 radiation pneumonitis, and most of them were asymptomatic and had only pneumonitis changes on CT images.

Spinal cord. A low dose to the spinal cord was maintained, because the use of beams that pass through the cord directly was intentionally avoided. The maximum dose in all patients was only 2.2 Gy per fraction. No patients showed cord toxicity.

Esophagus. The maximum dose to the esophagus in all patients was 5.2 Gy per fraction. The dose to the esophagus exceeded 5 Gy per fraction (20 Gy in total dose) only for the patient who showed the maximum dose. No severe esophageal toxicity greater than NCI-CTC Grade 2 was encountered.

Heart. The maximum dose to the heart in all patients was 10.6 Gy per fraction. The maximum volume of the heart irradiated over 5 Gy per fraction was 7.2 mL in the same patient. There were 5 patients whose maximum dose to the heart exceeded 5 Gy per fraction. In 3 of the 5 patients, more than 1 mL was irradiated with 5 Gy per fraction, and DVHs are shown in Fig. 6a. No severe cardiovascular toxicity greater than NCI-CTC Grade 2 was encountered.

Pulmonary artery. The maximum dose to the pulmonary artery in all patients was 11.2 Gy per fraction. The patient who showed the maximum dose to the pulmonary artery had a tumor near the pulmonary hilum. The volume irradiated

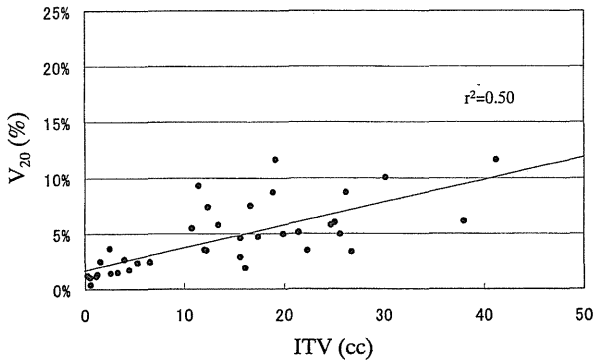

Fig. 5. Correlation with the internal target volume (ITV) and the volume irradiated with 20 Gy or more (V_{20}) of the lung. V_{20} had a tendency to increase as ITV increased ($r^2 = 0.50$). However, V_{20} also depended on the total lung volume and tumor position.

with 5 Gy or more was 5.13 mL, and the volume irradiated with 10 Gy or more was 0.86 mL in this patient. Dose to the pulmonary artery exceeded 5 Gy in 14 patients, the volume irradiated with 5 Gy or more exceeded 1 mL in 7 patients, whose DVH are shown in Fig. 6c. No clinical toxicity such as pulmonary bleeding or pulmonary artery obstruction was encountered.

Bronchus. Maximum dose to the bronchus in all patients was 7.9 Gy, and the maximum volume irradiated with 5 Gy or more was 2.92 mL. Figure 6b shows the DVH of the patient who was irradiated with the maximum dose to the bronchus. Though dose to the bronchus exceeded 5 Gy in 5 patients, the volume irradiated with 5 Gy or more did not exceed 1 mL except in the patient previously mentioned. No clinical toxicity such as symptomatic bronchitis or bronchial stenosis was encountered.

DISCUSSION

Stereotactic body frame was originally developed by Blomgren and Lax at Karolinska Hospital in Sweden (12, 13). It gives the following advantages: *(1)* Effective patient immobilization during treatment; *(2)* greater daily setup accuracy; *(3)* easy setup correction because of measuring scales on the frame; and *(4)* successful reduction of the respiratory tumor movement with a small abdominal pressing plate. Daily setup accuracy is much more important for SRT than for conventional radiotherapy, because a setup error in single treatment causes a larger error in total dose distribution. Its accuracy has been proven to be high enough in many articles, although verification and repositioning at every treatment are recommended (10, 12, 14). Its effectiveness on the reduction of respiratory tumor movement has also been proven in some articles (10, 14). On the other hand, this frame has the following disadvantages: excessive time required to arrange stereotactic coordinates; inappropriate application for obese patients; or limited availability of beam arrangement. The last disadvantage was considered an issue that should be solved before starting the practice of SRT with SBF. Therefore, we made the diagrams for available combinations of couch and gantry angles to use in routine clinics (11). We configured 5–10 noncoplanar beams using the diagrams, aiming for a practicable and balanced arrangement under the limitation. The diagrams were helpful in avoiding the selection of unusable beams in actual treatment.

We routinely use noncoplanar multiple static ports. The number of ports depends on the tumor size and location and is selected from 5 to 10 in our plan. Although a large number of ports makes dose distribution more conformal compared with a small number in general, our simulation revealed that it has made little difference in the increase of the number of ports more than 10 under the limitation of the couch and gantry arrangement. Moreover, because radiotherapy staff member enter the treatment room for checking that there is no collision when the gantry or the couch are moved, the large number of ports increases both treatment time and workload of the staff. These are the reasons why we use 5–10 static ports. Despite the limitation of the beam arrangement because of usage of the body frame and the supporting metal bar in the center of the couch, appropriate dose distributions were successfully achieved. Dose homogeneity indices for ITV were very small, and 90% dose coverage volumes were more than 99.5% in all cases except one.

The multiple arc technique is applied to SRT for extracranial tumors in a few institutes (15). However, there were some problems using this technique in our institute. Because the available beam range was limited by the SBF and couch structure, sufficient gantry rotational angles were not available. Also, the dose attenuation correction was practically impossible for an arc that contained both beams that passed and those that did not pass through the SBF. In our fundamental experiment for comparing the dose distribution between multiple static ports (6, 8, or 10 ports) and multiple arcs (3, 5, or 7 arcs, 300°), few differences were observed

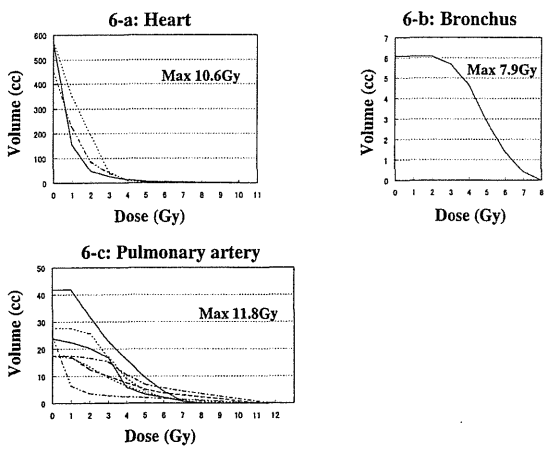

Fig. 6. Dose–volume histogram of the normal tissues. The dose–volume histogram of patients irradiated with more than 5 Gy to 1 mL or more of each normal tissue. (a) Heart. (b) Bronchus. (c) Pulmonary artery.

between both techniques in SRT for extracranial tumors under the constraints mentioned here. Therefore, we routinely use noncoplanar multiple static ports.

In regard to normal tissues, Emami *et al.* reported tolerance doses at a 5% complication rate in 5 years (TD 5/5) when irradiated with 2 Gy per fraction (16). This result, however, may not be applicable to hypofractionated, single, high-dose radiotherapy. Some recent articles reported on normal tissue complications in SRT for lung tumors. Severe toxicities are summarized in Table 3 (3, 4, 6, 13, 17). There are, however, few articles that have reported on the relationship between doses to normal tissues and their complications.

For lung doses, Graham *et al.* compared the total lung DVH parameters with the incidence and grade of pneumonitis after treatment for non–small-cell lung cancer. They concluded that V_{20} might be useful in comparing competing treatment plans to evaluate the risk of pneumonitis (18). We have used V_{20} of the total lung volume as a dose constraint for the lung. V_{20} was sufficiently lower than the dose constraint (25%) in our planning. We have encountered only 2 patients who showed radiation pneumonitis of Grade 2 in the NCI-CTC version 2.0, and no patients who showed Grade 3 or more. It is, however, controversial whether V_{20} can be applied to SRT in the same way as it is applied to conventional radiotherapy. We must follow this up carefully and analyze other parameters when severe toxicity occurs in the future.

A low dose to the esophagus was maintained in our planning, and no toxicity has yet been seen. Onimaru *et al.* have reported a patient who died because of a radiation-induced esophageal ulcer after receiving 48 Gy in eight fractions (6). The review of the planning revealed that 1 mL of the esophagus might have received 42.5 Gy with a maximum dose of 50.5 Gy. Though the case of this patient may have indicated the tolerance dose, they could not determine the essential maximum tolerance dose of the esophagus because of uncertainty in the contouring.

Wulf *et al.* reported fatal bleeding from the pulmonary artery 9 months after stereotactic irradiation (Grade 5) in a patient who received a previous conventional irradiation with a total dose of 60 Gy and stereotactic irradiation with a total dose of 30 Gy per 10 fractions. In our study, dose to the pulmonary artery was relatively higher when the tumor was located near the pulmonary hilum. Five Gy per fraction in more than 1 mL was irradiated in 5 of 7 patients. Severe toxicity has not yet been presented. The true volume of a pulmonary arterial wall irradiated with 5 Gy in the patients was smaller than the volume containing arterial blood used in our analysis. This might be one of the reasons why there has been no severe toxicity. However, the true tolerance dose to the pulmonary artery is still unknown.

Dose to the bronchus using brachytherapy has been reported to be from 4 to 6 Gy at a reference point per fraction with four fractionations in some typical protocols in other institutes. The reference point was typically located at a 5-mm depth from the mucosal surface, and more doses were irradiated at the mucosal surface. Our dose to the bronchus was considered to be much safer in comparison with these reports.

A low dose to the spinal cord was maintained in our planning because the use of the beam that included the spinal cord in the beam pathway was avoided. No patient with radiation myelitis has been reported after SRT. We changed the strategy of the beam arrangement and allowed just one of the beams to pass directly through the spinal cord in recent planning to improve the dose distribution for the target. One beam delivered a dose of about 2 Gy or less per fraction to the cord, when the fractional dose of 12 Gy was evenly delivered by six ports.

There is no report to be referred to regarding severe toxicity of the heart after stereotactic single high dose radiotherapy. In our study, although part of the heart was irradiated with a high dose in some patients, no severe complication has been encountered. However, the effect of high-dose irradiation to the coronary artery remains unclear, and the risk of severe toxicity may increase when a patient suffers from arterial atherosclerosis. Therefore, we must follow patients carefully over a long period. In regard to skin reaction, 7 patients (19%) showed erythema or pigmentation denoting Grade 1 acute toxicity at the entrance of a beam. No patient showed skin toxicity with Grade 2 or more.

Tolerance dose to OARs in SRT is a great concern for

Table 3. Severe toxicities (Grade 3 or more)

Authors	No. of targets (patients)	Dose/fraction at isocenter	Severe toxicities
Blomgren *et al.*	17 (13)	23–68 Gy/1–3 Fr.	Grade 3: Chronic cough (6%)
Hara *et al.*	23 (19)	20–30 Gy/1 Fr. (minimum to GTV)	Grade 3: Respiratory symptom (O_2 supply) (4%)
Onimaru *et al.*	57 (45)	48–60 Gy/8 Fr.	Grade 5: Esophageal ulcer (2%)
Wulf *et al.*	27	45 Gy/3 Fr.	Grade 3: Esophageal ulcer (4%) Grade 5: Pulmonary artery bleeding (4%)
Gomi *et al.*	38 (35)	40–62.5 Gy/4–5 Fr.	Grade 4: Pneumonitis (3%) Grade 4: Dermatitis (3%) Grade 3: Esophagitis (3%)

Abbreviations: Fr. = fraction; NCI-CTC = National Cancer Institute - Common Toxicity Criteria.

Severe toxicities of Grade 3 or more in NCI-CTC are summarized in this table. All of the authors in the table used three-dimensional conformal radiotherapy for lung tumors using hypofractionation or single fractionation shown in the table.